



Published in final edited form as:

Nature. 2008 October 30; 455(7217): 1268–1272. doi:10.1038/nature07298.

## Concurrent Nucleation of 16S Folding and Induced Fit in 30 S Ribosome Assembly

Tadepalli Adilakshmi<sup>1,3</sup>, Deepti L. Bellur<sup>2</sup>, and Sarah A. Woodson<sup>1,\*</sup>

<sup>1</sup> T.C. Jenkins Department of Biophysics, Johns Hopkins University, 3400 N. Charles St., Baltimore, MD 21218-2685 USA

<sup>2</sup> Program in Cell, Molecular and Developmental Biology and Biophysics, Johns Hopkins University, 3400 N. Charles St., Baltimore, MD 21218-2685 USA

### Summary

Rapidly growing cells produce thousands of new ribosomes each minute, in a tightly regulated process that is essential to cell growth.<sup>1,2</sup> How the 16S rRNA and 20 proteins that make up the 30S ribosomal subunit assemble faithfully in a few minutes remains a challenging problem, in part because real-time data on the earliest stages of assembly are lacking. Here, we show that 30S assembly nucleates concurrently from different points along the rRNA, by providing snapshots of individual RNA and protein interactions as they emerge in real time. Time-resolved hydroxyl radical footprinting<sup>3</sup> was used to map changes in the structure of the rRNA within 20 ms after addition of total 30S proteins. Helix junctions in each domain fold within 100 ms. By contrast, interactions surrounding the decoding site and between the 5', central and 3' domains require 2–200 seconds to form. Surprisingly, nucleotides contacted by the same protein are protected at different rates, indicating that initial RNA-protein encounter complexes refold during assembly. While early steps in assembly are linked to intrinsically stable rRNA structure, later steps correspond to regions of induced fit between the proteins and the rRNA.

---

Nomura and colleagues demonstrated that hierarchical addition of ribosomal proteins to the 16S rRNA produces cooperativity,<sup>4</sup> that is due to protein-induced structural changes in the 16S rRNA rather than direct contacts between proteins.<sup>5</sup> As the rRNA becomes more structured as proteins join the complex, assembly is coupled to the folding pathway of the rRNA.<sup>6,7</sup> The simplest kinetic model for 30S assembly is that regions of the 16S rRNA contacted by primary assembly proteins fold earliest, while helices stabilized by tertiary assembly proteins fold last. If assembly is strictly sequential, each subdomain of the rRNA will fold within a distinct time, producing a limited set of intermediate complexes.

Alternatively, the rate of protein binding may initially depend on the stochastic probability of forming locally stable rRNA and protein interactions, with progression to later intermediates depending on propagation of this conformational order to neighboring regions in the rRNA. If more than one region of the naked rRNA can fold, assembly is expected to nucleate from many places at once, producing an ensemble of reconstitution intermediates and multi-stage assembly kinetics.<sup>8</sup>

---

\*Corresponding author: E-mail: swoodson@jhu.edu, tel. +001-410-516-2015, FAX +001-410-516-4118.

<sup>3</sup>Present address: Weis Center for Research, Geisinger Medical Center, 100 North Academy Avenue, Danville, PA 17822

#### Author contributions

T. A. performed the experiments, analyzed the data, and prepared figures, D.L.B. analyzed protections in the 3' minor domain, S.A.W. prepared the figures and wrote the paper.

To visualize the intermediates of 30S ribosome assembly, the structure of the 16S rRNA was probed by time-resolved X-ray hydroxyl radical footprinting (Figure 1). The extent of RNA cleavage correlates with backbone exposure.<sup>9</sup> Thus, this method probes individual tertiary contacts in the rRNA as well as protein interactions that bury the rRNA backbone. Previous efforts to map the conformational changes in the 16S rRNA during 30S ribosome assembly used low temperature or subsets of proteins to stall assembly at specific stages.<sup>10,11</sup> We took advantage of the exceptional time resolution of synchrotron X-ray footprinting (~10 ms) to resolve the very early stages of assembly in real time, without needing to stall the reaction.

At the start of the experiment, native 16S rRNA from *E. coli* was prefolded at 42 °C in standard reconstitution buffer (see Methods; Figure 1a), as this pre-treatment improved the quality of reconstitution (Figure S2). Assembly of 30S ribosomal subunits was begun at 30 °C by mixing the rRNA with native total 30S proteins (TP30) using a rapid quench apparatus (see Methods). The rRNA-protein mixture was exposed to a white synchrotron X-ray beam for 10 ms to generate hydroxyl radical and cleave the exposed parts of the rRNA backbone.<sup>3</sup> The extent of cleavage at each position within the 16S rRNA was analyzed by primer extension and compared to parallel reactions on naked 16S rRNA and native 30S ribosomes (Figure 1b).

Many regions of the prefolded 16S rRNA were significantly protected from cleavage, indicating that the rRNA has native tertiary structure in the absence of proteins. This is consistent with chemical footprinting experiments<sup>5,10,12</sup> and with neutron scattering data showing that the deproteinized 16S rRNA has roughly the same dimensions as it does in the 30S ribosome.<sup>13</sup>

After a 3 min incubation with 30S proteins, the cleavage pattern was similar to that of native 30S ribosomes (Figure 1b), and correlated well with the solvent accessibility of the C4' atoms predicted from crystal structures of the *Thermus thermophilus* 30S<sup>14</sup> or *E. coli* 70S ribosomes.<sup>15</sup> Reconstitution of 30S subunits was confirmed by sedimentation velocity and activity assays (Supplemental Fig. S2). Additional rearrangements after 3 min may be needed to produce fully active subunits, as the temperature-dependent transition from RI to RI\* intermediates late in assembly is slow at 30 °C,<sup>16</sup> and is associated with changes in accessibility of the nucleobases rather than the backbone.<sup>11</sup> Nonetheless, most of the expected RNA and RNA-protein contacts formed within 3 minutes.

The kinetics of rRNA backbone protection revealed the presence of many assembly intermediates. Some nucleotides in the 16S rRNA were completely protected from hydroxyl radical cleavage within the 20 ms deadtime of our experiment, while others required 1–3 min to be fully protected (Figure 1c; Table S1). For many nucleotides, a partial burst of protection within the first 50–100 ms was followed by slower saturation of the contact over the next few minutes (Figures 1c and S3).

The multiphasic folding kinetics strongly indicates that individual 30S complexes take different routes to the final structure, as suggested by previously reported rates of protein binding<sup>17</sup> and by the kinetic partitioning of simple ribozymes among parallel folding pathways.<sup>18</sup> In kinetic footprinting experiments on the *Tetrahymena* ribozyme, partial protection of the RNA backbone at intermediate times was explained by the contemporaneous formation of folding intermediates with different structures.<sup>19</sup> We observed no exposure of 16S residues that might indicate the disappearance of non-native assembly intermediates over time. However, such interactions may have been too dynamic or heterogeneous to produce a distinct footprint.

To visualize the assembly pathway of the rRNA, the observed rate constants for making individual backbone contacts were clustered, and the clusters projected onto the secondary and tertiary structure of the mature 16S rRNA (Figure 2). This locates the interactions formed at each stage, even though the intermediate structures may differ from the mature structure.

Nucleotides with similar rates of backbone protection did not map to single domains, but were distributed throughout the 16S rRNA. In general, nucleotides that were protected in the first 20–50 ms (red; Figure 2) were partially folded in the naked rRNA or were protected by local structure such as a kink or a helix junction. Helices contacted by the primary assembly proteins S4 (5' domain), S7 (3' domain), S8 and S15 (central domain) were also protected within 50–100 ms after the proteins and rRNA were mixed. Thus, each domain assembles independently and simultaneously.

By contrast, the mRNA decoding site and long-range interactions between domains required the longest time to form (blue; Figure 2). For example, 16S helix H21 extends from the central domain to wrap around the body of the 30S subunit, where it contacts proteins S4 and S16. Interactions with H21 required 1 min to saturate completely ( $0.02$  to  $0.1$  s<sup>-1</sup>). The slow appearance of rRNA backbone contacts at G530 (H18) and the central pseudoknot (H2) in the decoding site is consistent with previous equilibrium studies demonstrating that structural changes in the central pseudoknot are linked to the transition from the RI to RI\* intermediates late in 30S assembly.<sup>11</sup>

The interplay between rRNA interactions that are intrinsically stable and those that are protein-dependent is illustrated by the kinetics of RNA and RNA-protein interactions in the body of the 30S ribosome (Figure 3a). H44 (3' minor domain) lies along one face of the body, packing against the stable tertiary structure formed by H7-H10 and H14.<sup>20</sup> Interactions with the distal tip of H44 are mediated by protein S20, which inserts its C-terminal  $\alpha$ -helix behind H8 and H14 in the 5' domain.<sup>21</sup> Many RNA tertiary interactions in the body of the 30S ribosome form within 20 ms (red; Figure 3a), while interactions with S20 form in 0.5 to 3 s (green), and long-range contacts with H44 form in ~10 s (blue). The multi-stage assembly of these RNA and protein interactions is consistent with the results of hydroxyl radical probing from Fe-EDTA complexes tethered to S20.<sup>22</sup>

We next asked whether the rates of RNA-protein interactions correlated with the position of each protein in the assembly map. Protections arising from direct protein-rRNA contacts were identified from crystallographic structures of the 30S ribosome<sup>21</sup> and previous footprinting of individual proteins<sup>23</sup> (see Supplemental Methods). Four of the six primary assembly proteins (S4, S7, S8, S15) protected a segment of their binding site during the first 50 ms of assembly. This was only true of three of the nine secondary assembly proteins (S16, S9, S10), and none of the tertiary assembly proteins (Table S2). Thus, primary assembly proteins were most likely to bind the rRNA early in assembly, in agreement with pulse-chase measurements of protein binding kinetics.<sup>17</sup>

Surprisingly, nucleotides contacted by a single protein were protected from hydroxyl radical cleavage with different rate constants (Figure 4). For example, protein S4 binds a five helix junction in the 5' domain, and initiates 30S assembly together with protein S7.<sup>24</sup> Interactions between S4 and 16S H17 (nt 436–441) saturated in 20–50 ms, while those in H3, H16, and H18 formed in 0.3 to 2 s, and those with H21 (nt 620) appeared over 8–10 s (Figure 4a). S7 binds a complex helix junction in the 16S 3' domain (Figure 4b).<sup>21</sup> H43 (nt 1369–1377) was protected in 20–50 ms, while contacts with H29, H41 and the distant H37 were protected more slowly. Thus, S4 and S7 engage their binding sites in stages rather than in one step. Similar behavior was observed for proteins S8, S9, S10, S15 and S16 (Figures S4 and S5).

The unexpectedly complex kinetics of the rRNA-protein interactions can be explained by the formation of encounter complexes that slowly reorganize into the final complex. For S4, the variable kinetics of rRNA backbone protection may be due to co-folding of the protein and the rRNA.<sup>25</sup> H17, which is protected rapidly, contacts the well-folded CTD of S4.<sup>21</sup> By contrast,

H18 and the top of H16, which are protected at an intermediate rate, contact the S4 NTD, which is disordered in solution.<sup>26</sup>

If different regions of the 16S rRNA fold and interact with the ribosomal proteins simultaneously, how can we understand the hierarchy of protein association represented by the assembly map? The association rates implied by the fastest rates of RNA backbone protection approach the diffusion-controlled limit ( $10^8 \text{ M}^{-1}\text{s}^{-1}$ ). However, the slowest protection rates are most similar to the protein binding rates measured by pulse-chase mass spectrometry<sup>17</sup> (Table S2). Our data suggest that slow forming interactions in the rRNA, many of which are indirectly stabilized by bound proteins, determine the rate of protein addition and the hierarchy of assembly.

This idea is illustrated by interactions of protein S7, which is necessary for stable binding of other proteins to the 16S 3' domain.<sup>24,27</sup> Residues indirectly protected by S7,<sup>23</sup> which overlap the binding sites of the secondary assembly proteins S9, S13 and S19, fold slowly (Figure S5), explaining why these proteins join 30S complexes more slowly than S7.<sup>17</sup> However, residues in H34 that directly contact S9 and S10 are fully protected in 50 ms (Figures 3b and S5). Thus, S7, S9 and S10 all engage their binding sites in the rRNA early in assembly, but productive incorporation of S9 and S10 presumably waits for conformational changes in the 16S rRNA induced by S7. An important question is whether early stochastic interactions between the ribosomal proteins and the rRNA backbone bias the ensemble of rRNA conformations towards the native state, thus accelerating self-assembly, or whether these interactions delay the search for the native conformation.

In conclusion, stable structure in the 16S rRNA allows the concurrent nucleation of assembly from many points along the rRNA, resulting in the seemingly chaotic but rapid appearance of native interactions throughout the complex. Previous studies indicated that ribosome assembly is not completely cooperative,<sup>28</sup> implying the need for multiple nucleation sites.<sup>2</sup> The lack of complete cooperativity and differences between the time-dependence of 16S folding and the assembly map revealed by kinetic footprinting of the nucleobases<sup>10</sup> support the conclusion that assembly proceeds in parallel through intermediates with different subsets of proteins.<sup>6,8</sup> *In vivo*, assembly of the pre-rRNA during transcription is more cooperative and involves specific accessory factors.<sup>6,8</sup> Co-transcriptional assembly may simplify the pathway by limiting the number of intermediates that can be populated. Nonetheless, we expect stochastic fluctuations among alternative intermediates to contribute to the early pathway of ribosome assembly *in vivo*.

## Methods Summary

Native *E. coli* 16S rRNA was prefolded in 80 mM K-cacodylate, pH 7.5, 330 mM KCl, 20 mM MgCl<sub>2</sub> for 15 min at 42 °C, then mixed with an equal volume of *E. coli* TP30 in the same buffer, at 30 °C, using a Kin-Tek rapid quench apparatus fitted with an X-ray flow cell. 20–40% of the input RNA was cleaved after 10 or 20 ms exposure to a white light synchrotron beam (X28C, NSLS, Brookhaven National Laboratory). The cleaved RNA was analyzed by primer extension with reverse transcriptase. The increase in relative backbone protection (*Y*) after the addition of TP30 was fit to rate equations to obtain observed rate constants and amplitudes for the reaction (see Supplemental Figures and Tables). Individual protections were assigned to specific RNA or RNA-protein interactions, based on crystallographic structures (pdb 1j5e,<sup>15</sup> 2avw and 2avy<sup>15</sup>); see full methods for details.

## Supplementary Material

Refer to Web version on PubMed Central for supplementary material.

## Acknowledgments

The authors thank R. Moss, A. Cukras, L. Cochella and R. Green for help with ribosome preparation and peptidyl transferase assays, P. Fleming for help with Calc-Surf software and S. Gupta, M. Sullivan and M. Brenowitz for help with X-ray footprinting. This work was supported by the NIH (GM60819), NSLS X28C and the Center for Synchrotron Biosciences are supported by NIH P41-EB0001979.

## References

1. Warner JR, Vilardell J, Sohn JH. Economics of ribosome biosynthesis. *Cold Spring Harb Symp Quant Biol* 2001;66:567–74. [PubMed: 12762058]
2. Nierhaus KH. The assembly of prokaryotic ribosomes. *Biochimie* 1991;73:739–55. [PubMed: 1764520]
3. Ralston CY, et al. Time-resolved synchrotron X-ray footprinting and its application to RNA folding. *Methods Enzymol* 2000;317:353–68. [PubMed: 10829290]
4. Held WA, Mizushima S, Nomura M. Reconstitution of *Escherichia coli* 30 S ribosomal subunits from purified molecular components. *J Biol Chem* 1973;248:5720–30. [PubMed: 4579428]
5. Stern S, Powers T, Changchien LM, Noller HF. RNA-protein interactions in 30S ribosomal subunits: folding and function of 16S rRNA. *Science* 1989;244:783–790. [PubMed: 2658053]
6. Culver GM. Assembly of the 30S ribosomal subunit. *Biopolymers* 2003;68:234–49. [PubMed: 12548626]
7. Williamson JR. After the ribosome structures: how are the subunits assembled? *RNA* 2003;9:165–7. [PubMed: 12554857]
8. Noller, HF.; Nomura, M. *Escherichia coli* and *Salmonella typhimurium*, cellular and molecular biology. Neidhardt, FC., editor. American Society for Microbiology; Washington, D. C: 1987. p. 104-125.
9. Tullius TD, Greenbaum JA. Mapping nucleic acid structure by hydroxyl radical cleavage. *Curr Opin Chem Biol* 2005;9:127–34. [PubMed: 15811796]
10. Powers T, Daubresse G, Noller HF. Dynamics of in vitro assembly of 16 S rRNA into 30 S ribosomal subunits. *J Mol Biol* 1993;232:362–374. [PubMed: 8345517]
11. Holmes KL, Culver GM. Mapping structural differences between 30S ribosomal subunit assembly intermediates. *Nat Struct Mol Biol* 2004;11:179–86. [PubMed: 14730351]
12. Adilakshmi T, Ramaswamy P, Woodson SA. Protein-independent folding pathway of the 16S rRNA 5' domain. *J Mol Biol* 2005;351:508–19. [PubMed: 16023137]
13. Ramakrishnan V. Distribution of protein and RNA in the 30S ribosomal subunit. *Science* 1986;231:1562–4. [PubMed: 3513310]
14. Wimberly BT, et al. Structure of the 30S ribosomal subunit. *Nature* 2000;407:327–339. [PubMed: 11014182]
15. Schuwirth BS, et al. Structures of the bacterial ribosome at 3.5 Å resolution. *Science* 2005;310:827–34. [PubMed: 16272117]
16. Traub P, Nomura M. Structure and function of *Escherichia coli* ribosomes. VI. Mechanism of assembly of 30 s ribosomes studied in vitro. *J Mol Biol* 1969;40:391–413. [PubMed: 4903714]
17. Talkington MW, Siuzdak G, Williamson JR. An assembly landscape for the 30S ribosomal subunit. *Nature* 2005;438:628–32. [PubMed: 16319883]
18. Pan J, Thirumalai D, Woodson SA. Folding of RNA involves parallel pathways. *J Mol Biol* 1997;273:7–13. [PubMed: 9367740]
19. Laederach A, Shcherbakova I, Liang MP, Brenowitz M, Altman RB. Local kinetic measures of macromolecular structure reveal partitioning among multiple parallel pathways from the earliest steps in the folding of a large RNA molecule. *J Mol Biol* 2006;358:1179–90. [PubMed: 16574145]
20. Cate JH, Yusupov MM, Yusupova GZ, Earnest TN, Noller HF. X-ray crystal structures of 70S ribosome functional complexes. *Science* 1999;285:2095–2104. [PubMed: 10497122]
21. Brodersen DE, Clemons WM Jr, Carter AP, Wimberly BT, Ramakrishnan V. Crystal structure of the 30 S ribosomal subunit from *Thermus thermophilus*: structure of the proteins and their interactions with 16 S RNA. *J Mol Biol* 2002;316:725–68. [PubMed: 11866529]

22. Dutca LM, Culver GM. Assembly of the 5' and 3' minor domains of 16S ribosomal RNA as monitored by tethered probing from ribosomal protein S20. *J Mol Biol* 2008;376:92–108. [PubMed: 18155048]
23. Powers T, Noller HF. Hydroxyl radical footprinting of ribosomal proteins on 16S rRNA. *RNA* 1995;1:194–209. [PubMed: 7585249]
24. Nowotny V, Nierhaus KH. Assembly of the 30S subunit from *Escherichia coli* ribosomes occurs via two assembly domains which are initiated by S4 and S7. *Biochemistry* 1988;27:7051–5. [PubMed: 2461734]
25. Powers T, Noller HF. A temperature-dependent conformational rearrangement in the ribosomal protein S4.16 S rRNA complex. *J Biol Chem* 1995;270:1238–1242. [PubMed: 7836385]
26. Sayers EW, Gerstner RB, Draper DE, Torchia DA. Structural preordering in the N-terminal region of ribosomal protein S4 revealed by heteronuclear NMR spectroscopy. *Biochemistry* 2000;39:13602–13. [PubMed: 11063598]
27. Samaha RR, O'Brien B, O'Brien TW, Noller HF. Independent in vitro assembly of a ribonucleoprotein particle containing the 3' domain of 16S rRNA. *Proc Natl Acad Sci U S A* 1994;91:7884–8. [PubMed: 8058729]
28. Dodd J, Kolb JM, Nomura M. Lack of complete cooperativity of ribosome assembly in vitro and its possible relevance to in vivo ribosome assembly and the regulation of ribosomal gene expression. *Biochimie* 1991;73:757–67. [PubMed: 1764521]

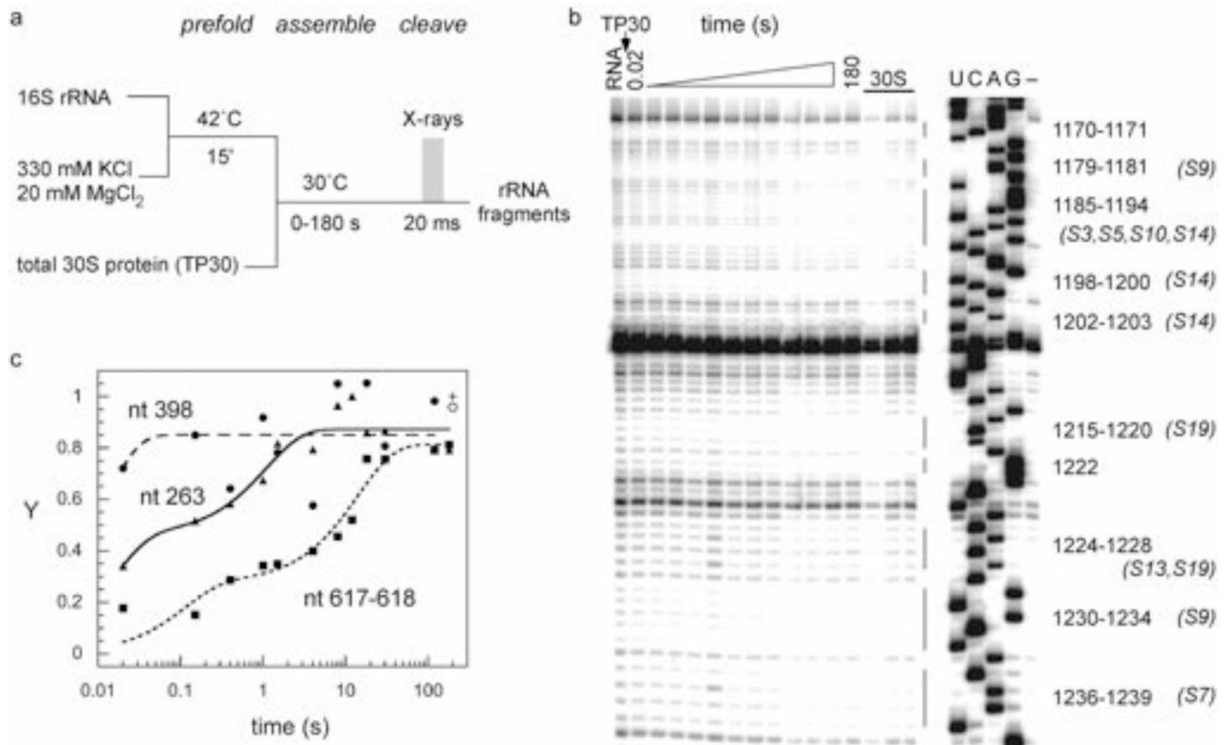


**Figure 1. Time-resolved X-ray footprinting of 30S ribosome assembly**

**a**, Native 16S rRNA and total protein from 30S subunits (TP30) were mixed in 5–10 ms and irradiated with a synchrotron X-ray beam, to cleave the RNA at exposed riboses. **b**, 16S fragments were analyzed by primer extension. Cleavage pattern 0.02 to 180 s post-TP30. RNA, pre-folded 16S rRNA; 30S, triplicate controls on native 30S subunits; UCAG, dideoxy sequence ladders; –, untreated RNA. Primer anneals after nt 1257. **c**, Relative saturation (Y) of each protection vs. assembly time, fit to single or double exponential rate equations (Supplemental Methods). (●), nt 398; (▲), nt 263; (■), nt 617–618; (○,+), average of 30S controls. Additional data are in Figure S3 and Table S1.

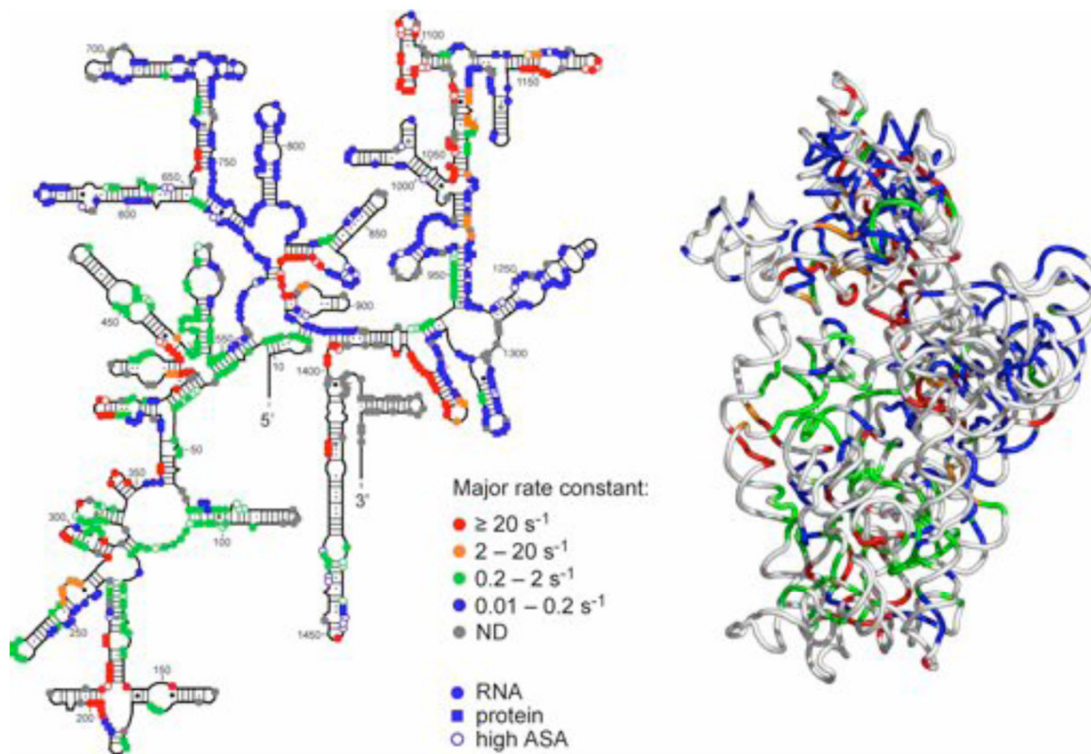


**Figure 2. Simultaneous folding of 16S domains**

**a**, Protected nucleotides (740 positions) were clustered according to the rate (time) constant for backbone protection and colored as indicated in the key. Where the amplitude of the initial burst phase is  $\leq 60\%$ , the slower rate constant is used. Grey (120 positions), rate constant undetermined due to a pause in reverse transcription or weak protection. Natural adenine methylation hampered quantitative analysis of residues in the decoding site. Circles, RNA-RNA contact; square, RNA-protein contact; solid symbols, buried C4' in crystal structures, open circles, predicted C4' ASA  $> 4 \text{ \AA}^2$ . **b**, 3D ribbon of *E. coli* 16S rRNA (2awy)<sup>15</sup> colored as in **a**, viewed from the 50S interface. See Figure S4 for additional views of each domain.



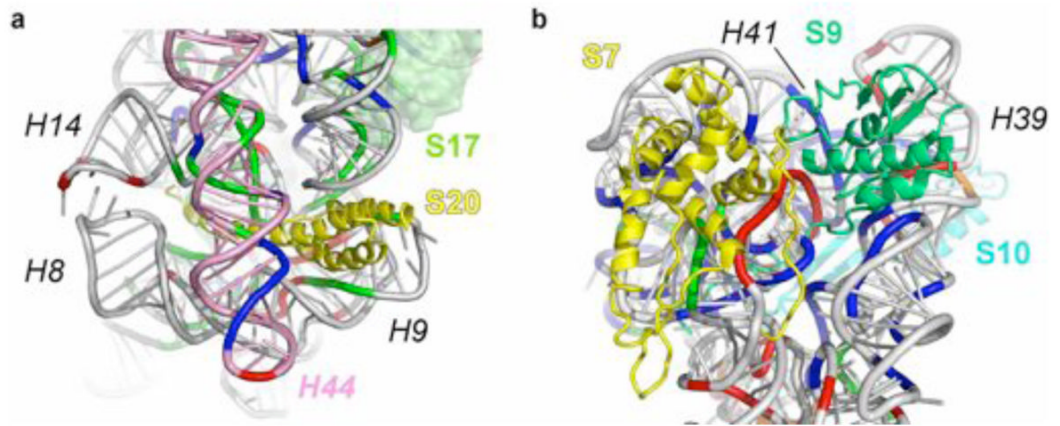


**Figure 3. Stepwise assembly of RNA and protein interactions**

**a.** Protein S20 (yellow ribbon) contacts the 30S body (5' domain; grey) earlier than helix 44 in the 3' minor domain (pink). 16S nts colored as in Figure 2. **b.** Proteins S7 (yellow) and S9 (green) protect a segment of their binding site immediately (red), while nucleotides at the interface between the subdomains are protected slowly (blue).

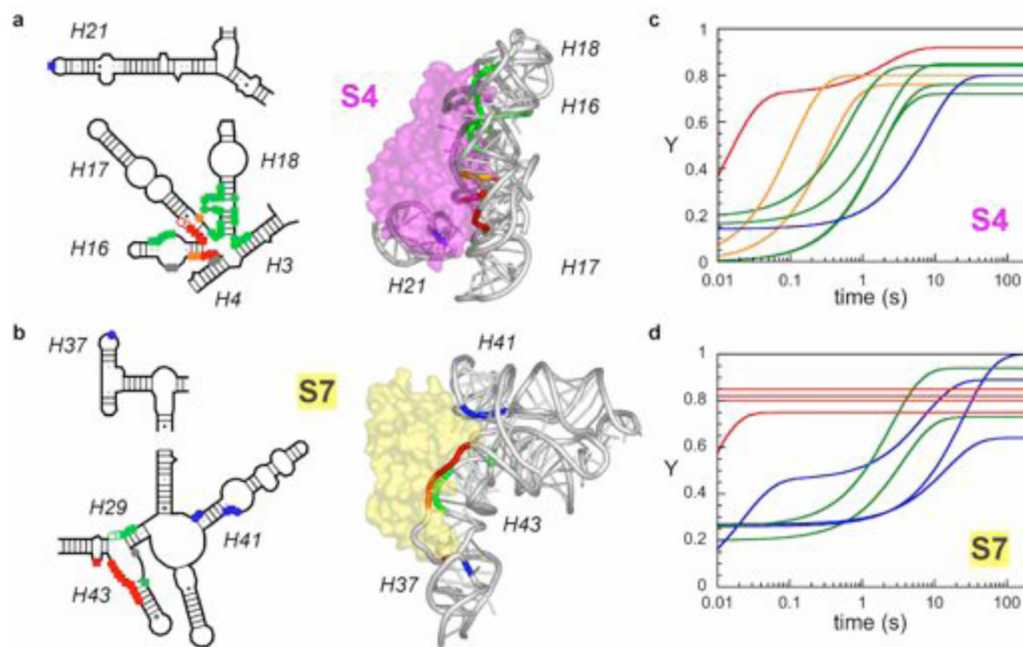


**Figure 4. Ribosomal proteins interact with the rRNA in stages**  
**a, b,** Kinetics of direct rRNA backbone protection by protein S4 (magenta) and S7 (yellow), colored as in Figure 2. Schematic symbols also as in Figure 2. **c, d,** Progress curves for protection of individual residues in contact with S4 and S7; for clarity only fitted curves are shown (see data in Figure S5). See Supplemental Methods for definition of RNA-protein contacts.